electronic materials

MDPI

Communication

Experimental Evaluation of Hole Mobility in Organic Semiconductors Based on Benzo[*f*][1,2,5]oxadiazolo[3,4-*b*]thieno[3,2-*h*]quinoxalines

Alexander S. Steparuk [1], Elizaveta M. Krynina [1], Yuriy A. Kvashnin [1], Pavel A. Slepukhin [1,2], Kristina E. Nevezhina [3], Alexey V. Ishchenko [3], Ilya A. Weinstein [3], Egor V. Verbitskiy [1,*] and Valery N. Charushin [1,2]

[1] I. Ya. Postovsky Institute of Organic Synthesis, Ural Branch of the Russian Academy of Sciences, S. Kovalevskaya Str., 22, 620137 Ekaterinburg, Russia
[2] Department of Organic and Biomolecular Chemistry, Ural Federal University, Mira St. 19, 620002 Ekaterinburg, Russia
[3] NANOTECH Center, Ural Federal University, Mira St. 19, 620002 Ekaterinburg, Russia
* Correspondence: verbitskye@yandex.ru

Abstract

For the first time, the hole mobility values for benzo[*f*]- and naphtho[1,2-*f*]-annelated [1,2,5]oxadiazolo[3,4-*b*]thieno[3,2-*h*]quinoxalines were determined experimentally by using the space-charge-limited current method. Analysis of the X-ray diffraction data for naphtho[1,2-*f*][1,2,5]oxadiazolo[3,4-*b*]thieno[3,2-*h*]quinoxaline revealed significant π–π stacking, which may be attributed to enhanced electron mobility. These findings are further supported by the observed low hole conductivity values, which reached 4.10×10^{-9} $cm^2 \cdot V^{-1} \cdot s^{-1}$. Therefore, polycyclic compounds based on the furazano[3,4-*b*]pyrazine core can be considered a convenient scaffold for developing both electron and hole transport materials in various organic photovoltaic devices.

Keywords: furazano[3,4-*b*]pyrazines; 1,4-diazatriphenylenes; polycyclic systems; organic semiconductors

1. Introduction

In the past decade, organic electronics has emerged as a groundbreaking technology that leverages the unique structural and functional properties of carbon-based semiconductors [1]. Unlike traditional inorganic semiconductor materials, such as silicon or metal-oxide systems, organic electronic materials made from small molecules or polymers offer several advantages. These materials often exhibit mechanical flexibility, biocompatibility, solution-based process ability, and the capacity to tune optoelectronic properties through careful molecular design. Today, modern organic electronic materials are used in a wide variety of applications, including wearable sensors, foldable displays, biointegrated devices, and systems for sustainable energy generation and storage [2–7]. (Hetero)polycyclic aromatic hydrocarbons belong to the family of planar conjugated compounds and can be described as heterocyclic analogs of discrete sections of graphene sheets, making them particularly interesting for organic electronic applications [8–11]. A noteworthy compound in this area is 1,4-diazatriphenylene, also known as dibenzo[*f*,*h*]quinoxaline, along with its heterofused analogs [12–14]. These polycyclic nitrogen-containing heteroaromatic compounds are characterized by fully conjugated frameworks that are forced to be planar and feature

Check for updates

Academic Editor: Wojciech Pisula

Received: 3 August 2026
Revised: 7 September 2026
Accepted: 9 September 2026
Published: 10 September 2026

Copyright: © 2026 by the authors. Licensee MDPI, Basel, Switzerland. This article is an open access article distributed under the terms and conditions of the Creative Commons Attribution (CC BY) license.

threefold rotational symmetry. They have become essential building blocks in advanced materials chemistry and various optoelectronic devices, functional coordination polymers, and energy storage systems. Among the hetero-fused analogs of 1,4-diazatriphenylene, the most promising derivatives are those based on the [1,2,5]oxadiazolo[3,4-*b*]pyrazine scaffold, also known as furazano[3,4-*b*]pyrazine [15–20]. Recent research studies have demonstrated a high potential for using push–pull (**I** and **II**) and polycyclic (**III**) systems of the family of furazano[3,4-*b*]pyrazines as electron and (Figure 1) hole transport layers in organic light-emitting diodes (OLEDs) and perovskite solar cells [21–23]. Notably, the best measurement data obtained for dibenzo[*f*,*h*]furazano[3,4-*b*]quinoxalines (**III**) in thin films have indicated a level of experimental hole mobility of approximately ~10^{-4} $cm^2 \cdot V^{-1} \cdot s^{-1}$ [23]. It was suggested that the widely used and commercially available 2,2′,7,7′-*tetrakis*[*N*,*N*-di(4-methoxyphenyl)amino]-9,9′-spirobifluorene (**Spiro-MeOTAD**) has a hole mobility of 8.5×10^{-7} $cm^{-2} \cdot V^{-1} \cdot s^{-1}$ (Figure 1) [24]. However, more recent experimental data presented in the review [25] show that the hole mobility of **Spiro-MeOTAD** is on the order of 10^{-4} $cm^{-2} \cdot V^{-1} \cdot s^{-1}$. Therefore, the hole mobility values obtained for polycyclic systems (**III**) can be considered comparable to those for **Spiro-MeOTAD**.

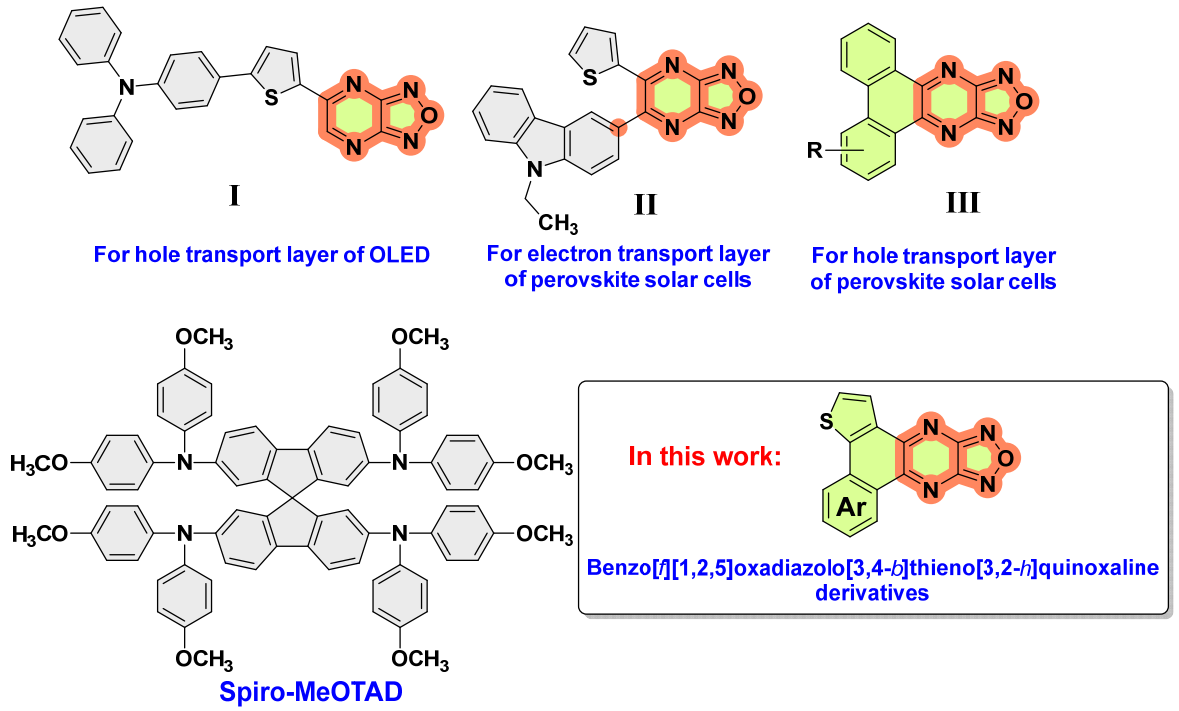


Figure 1. Representative organic semiconductors based on the previously obtained furazano[3,4-*b*]pyrazines and the standard hole semiconductor **Spiro-MeOTAD**.

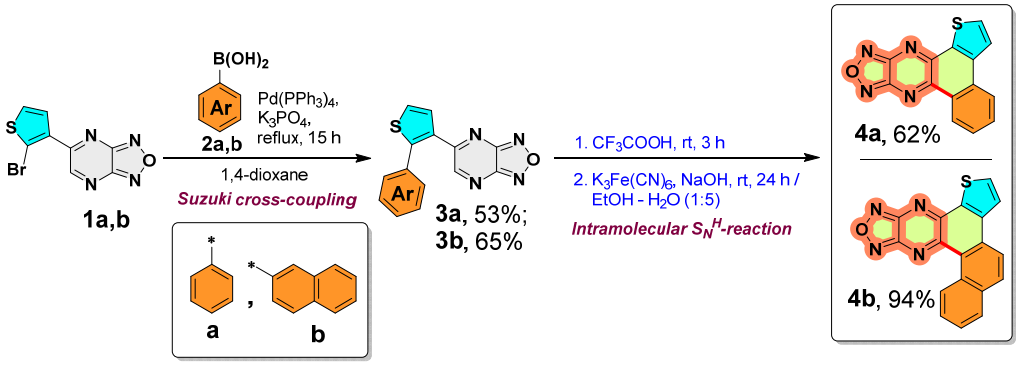
In continuation of our research studies on this promising family of organic semiconductors, we present this communication with the data on the experimental evaluation of hole mobility values for benzo[*f*][1,2,5]oxadiazolo[3,4-*b*]thieno[3,2-*h*]quinoxaline and naphtho[1,2-*f*][1,2,5]oxadiazolo[3,4-*b*]thieno[3,2-*h*]quinoxaline. These values were determined experimentally by using the space-charge-limited current method. Additionally, we have analyzed the X-ray diffraction data for these polycyclic compounds to help rationalize our findings.

2. Materials and Methods

All reagents and solvents were obtained from commercial sources and dried before use according to standard procedures. Molybdenum(VI) oxide (MoO_3) (≥99.5%) was

purchased from the company Khimkraft (Russia, Kaliningrad, https://xn--80apghvnnc.xn--p1ai/, 25 May 2026). Aluminum was purchased from Component-Reaktiv (Russia, Moscow, https://www.component-reaktiv.ru/, https://xn--80apghvnnc.xn--p1ai/, 25 May 2026). Poly(3,4-ethylenedioxythiophene)-poly(styrenesulfonate) (PEDOT:PSS, 1.48% aqueous dispersion) was purchased from BLD Pharm (China, Shanghai, https://www.bldpharm.com/products/155090-83-8.html, https://xn--80apghvnnc.xn--p1ai/, 25 May 2026).

Compounds **4a** and **4b** have been synthesized (Scheme 1) through the procedure described earlier [22].



Scheme 1. Synthesis of benzo[*f*][1,2,5]oxadiazolo[3,4-*b*]thieno[3,2-*h*]quinoxaline derivatives (**4a**,**b**).

The general details of the X-ray experiment as well as fabrication and characterization of hole-only devices, analytical equipment and methods are provided in the Supplementary Materials.

3. Results

3.1. Synthesis and X-Ray Diffraction Data

In a previously developed strategy that combines nucleophilic aromatic substitution of hydrogen (S_N^H) and transition metal-catalyzed cross-coupling reactions [26], we have successfully designed and synthesized for the first time novel heteropolycyclic systems of the family of benzo[*f*][1,2,5]oxadiazolo[3,4-*b*]thieno[3,2-*h*]quinoxaline. Their synthesis was based on using the readily available starting material, 5-(2-bromothiophen-3-yl)-[1,2,5]oxadiazolo[3,4-*b*]pyrazine (**1**). This compound undergoes the Suzuki cross-coupling reaction with the corresponding boronic acids, followed by an intramolecular S_N^H-reaction, resulting in the target products **4a**,**b** in yields up to 94% (Scheme 1) [22].

While the purity and structure of products **4a**,**b** were established previously through ^{1}H and ^{13}C NMR spectroscopy and elemental analysis, this study allowed us to obtain the X-ray diffraction data for a single crystal of **4b**. According to the XRD data, compound **4b** crystallizes in the centrosymmetric space group of the monoclinic system. The general geometry of the molecules is shown in Figure 2a. The molecule **4b** is planar within 0.150 Å. The bond distances and angles in the molecule are close to the expected values. The molecular packing in the crystal is layered; the molecules are oriented in the plane (102) (Figure 2b). Between molecules **4b**, shortened contacts are observed with the distance between planes of the nearest molecules approximately 3.4 Å and shortened interatomic C…C contacts 3.36 Å (Figure 2c), which are typical for polycyclic compounds bearing the furazano[3,4-*b*]pyrazine core [20,23], and are close to the layer distance in graphite (3.35 Å) [27]. This is characteristic of a pronounced $\pi-\pi$ interaction between two aromatic fragments. In fact, very poor solubility was observed for **4b**, thus indicating strong $\pi-\pi$ interactions [28]. All these findings suggest that polycyclic compound **4a** may also possess strong intermolecular $\pi-\pi$ stacking interactions.

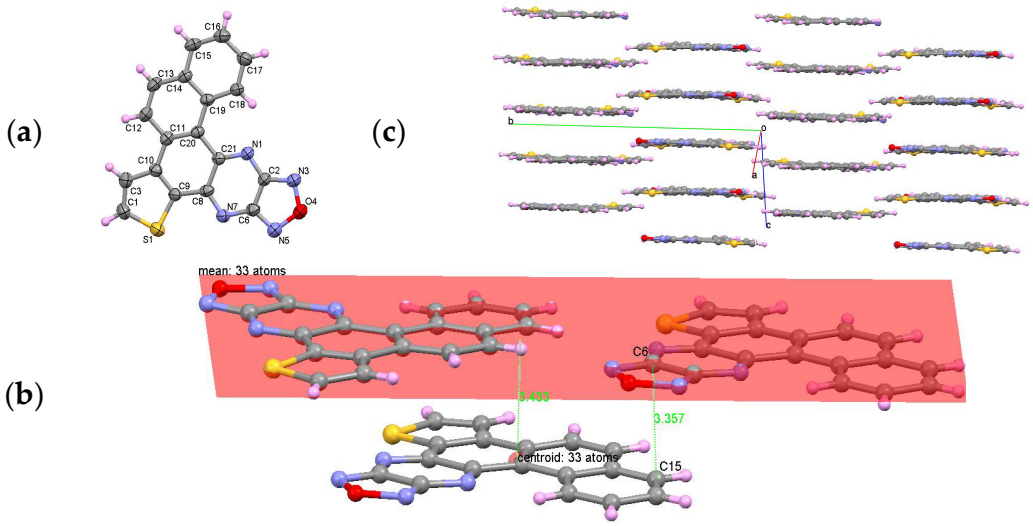


Figure 2. (**a**) ORTEP of **4b** with thermal ellipsoids at the 50% probability level; (**b**) molecular packing for **4b** in the plane (102); (**c**) fragment of stack with interfacial distances in Å.

3.2. Photophysical and Charge Transport Properties

(Hetero)polycyclic compounds **4a**,**b** are red-brown, non-luminescent solids with absorption maxima ranging from 255 to 440 nm (Table 1). Keeping in mind information concerning the data of electrochemical studies regarding frontier orbital energies and the charge transport properties of [1,2,5]oxadiazolo[3,4-*b*]pyrazine derivatives (**I**–**III**) [21–23], hole-only devices with an ITO/PEDOT:PSS/Polycycle **4a** (or **4b**)/MoO_3 (25 nm)/Al (100 nm) structure were fabricated (Figure 3a,b). These devices were employed to investigate charge carrier mobility using the space-charge-limited current (SCLC) method. The hole-only device is typically constructed as a sandwich with a hole transport layer positioned between two electrodes. In this device, glass slices are used as the substrate, indium tin oxide (ITO) serves as the anode, and aluminum (Al) functions as the cathode [29]. The polymeric compound, namely poly(3,4-ethylene dioxythiophene)/poly(styrene-sulfonate) (PEDOT/PSS), which has a work function of approximately 5.1 eV, acts as a conducting layer that enables hole injection into the HOMO of an electron-donating organic material with a similar work function of about ~5.5 eV [30]. MoO_3 serves as a hole-transporting/electron-blocking interlayer with a work function of approximately −5.3 eV [31]. This value is significantly lower than the lowest unoccupied molecular orbital (LUMO) energy of polycyclic compounds **4a** and **4b**, which is around -4.2 ± 0.1 eV (Table 1) [22]. As a result, this difference effectively prevents electron injection into the device. When a sufficient voltage is applied to the hole-only device, hole transport through the polycyclic compound **4** film becomes limited by the accumulated space charge. In this case, the space-charge-limited current can be described by the well-known Mott–Gurney equation, which describes the current–voltage relation (see Equation (1)) [32],

$$J = \frac{9\varepsilon_0\varepsilon_r\mu_h V^2}{8L^3} \quad (1)$$

where ε_0 is the vacuum permittivity, ε_r is the permittivity of the electron-donating organic material (ε_r = 3), μ_h is the hole mobility, V is the applied voltage, and L is the thickness of the electron-donating organic material layer. In the calculations of charge carrier mobility, the applied voltage (V_{appl}) is corrected for the effect of the "build-in field", $V = V_{appl} - V_{bi}$, where V_{bi} (build-in potential) is the difference between the work functions of PEDOT:PSS and Al. The current–voltage curves for the fabricated devices are displayed in Figure 4a,b. According to Equation (1), current density is proportional to the square of the voltage

(J~V^2). To linearize this quadratic relationship, we plotted the experimental data in the coordinates of $J^{1/2}$ versus V_{appl}–V_{bi}. The resulting linear behavior confirms the validity of the Mott–Gurney model and enables the direct calculation of carrier mobility (μ_h) from the slope of the line. The high quality of the linear fit ($R^2 > 0.99$) highlights the reliability of the extracted parameters.

Table 1. Optical, electrochemical [1] and hole mobility data for benzo[*f*][1,2,5]oxadiazolo[3,4-*b*]thieno[3,2-*h*]quinoxaline derivatives (**4a**,**b**).

Compound	λ_{abs}, nm/ ($\varepsilon \times 10^3$, $M^{-1}\cdot cm^{-1}$)	E_{Ox}^{onset}, eV	E_{Red}^{onset}, eV	E_{HOMO}, eV	E_{LUMO}, eV	E_g^{el}, eV	Hole Mobility ($cm^2\cdot V^{-1}\cdot s^{-1}$)
4a	285/51.7 295/62.5 370/36.1	1.05	−0.20	−5.49	−4.24	1.25	4.10×10^{-9}
4b	255/33.8 315/14.9 440/13.7	-	−0.18	-	−4.26	-	1.85×10^{-6}

[1] The optical and electrochemical properties of compounds **4a**,**b** were previously described in detail in reference [22].

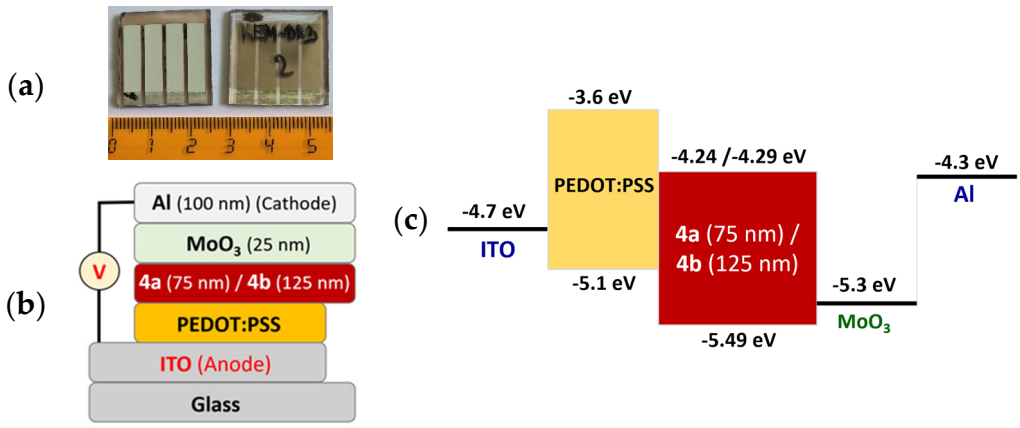


Figure 3. (**a**) Photo of hole-only device cells; (**b**) the basic structure of the hole-only device; (**c**) the energy structure of the hole-only device.

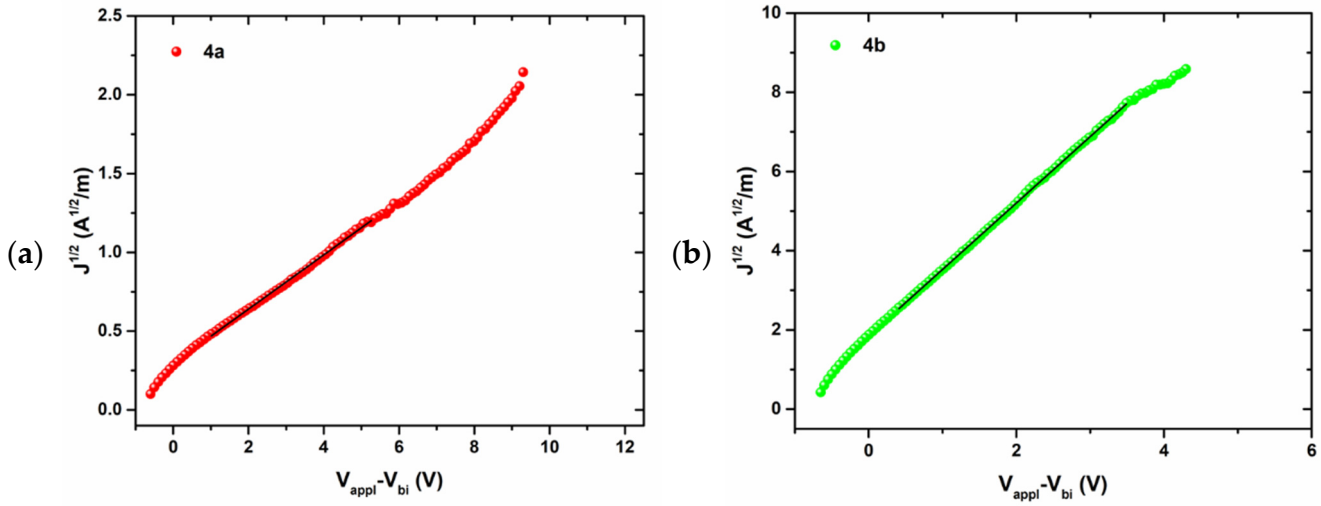


Figure 4. The dependences $J^{1/2}$ V for a hole-only device based on **4a** (**a**) and **4b** (**b**).

Based on the current–voltage characteristics, the drift mobility of the device using polycyclic compound **4a** was measured to be 4.10×10^{-9} $cm^2 \cdot V^{-1} \cdot s^{-1}$. In contrast, compound **4b** exhibited a significantly higher charge carrier mobility of 1.85×10^{-6} $cm^2/V \cdot s$, nearly three orders of magnitude greater than that of **4a**. The significant increase in charge carrier mobility upon moving from compound **4a** to **4b** appears to be attributed to the structural features of polycyclic systems. Modifying the structure by introducing an extended naphthalene bicyclic system in place of the benzene ring expands the π-conjugated system, which may facilitate more efficient delocalization of charge carrier wave functions and reduce the internal energy of molecular reorganization upon their transition to a charged state. Additionally, the expansion of the aromatic framework is likely to have a significant impact on the supramolecular organization in the solid phase. The published data [33–35] on similar condensed heterocyclic systems indicate that an increase in the area of the planar scaffold promotes a change in the geometry of intermolecular packing within thin films. Specifically, this change involves a transition from a less efficient herringbone-type packing to a denser layer-by-layer π–π stacking arrangement. The closer alignment of molecular planes and the increased overlap of orbitals between adjacent molecules substantially reduce the energy barriers for charge transport within the semiconductor bulk. This is evidenced by a notable increase in macroscopic drift mobility, as measured by the SCLC method.

The energies of the highest occupied molecular orbital (HOMO) and the lowest unoccupied molecular orbital (LUMO) play a critical role in determining the electronic and conductive properties of materials. There is a direct relationship between the types of charge carriers in organic thin-film transistors and the experimentally measured levels of frontier molecular orbitals [36]. The literature indicates that materials with a LUMO energy lower than −3.15 eV and a HOMO energy higher than −5.60 eV can demonstrate both *p*-type and *n*-type (ambipolar) semiconductor behavior [36].

As shown in Table 1 and reference [22], benzo[*f*][1,2,5]oxadiazolo[3,4-*b*]thieno[3,2-*h*]quinoxalines (**4a**,**b**) are expected to exhibit typical ambipolar semiconductor properties based on their HOMO and LUMO energies. This expectation is indirectly supported by the sharp decrease in *p*-type conductivity to approximately 10^{-9} $cm^2 \cdot V^{-1} \cdot s^{-1}$. Unfortunately, we were unable to obtain experimental data on the electron conductivity of these compounds due to a lack of technical resources.

4. Conclusions

The hole mobility values for thin films made from benzo[*f*][1,2,5]oxadiazolo[3,4-*b*]thieno[3,2-*h*]quinoxaline derivatives were experimentally determined for the first time by using the space-charge-limited current method. The analysis of X-ray diffraction data, along with the energies of the HOMO and LUMO for naphtho[1,2-*f*][1,2,5]oxadiazolo[3,4-*b*]thieno[3,2-*h*]quinoxaline revealed significant π–π stacking, which strongly contributes to its electron conductivity. However, it demonstrated a very low hole conductivity, in the range of approximately 10^{-6} to 10^{-9} $cm^2 \cdot V^{-1} \cdot s^{-1}$. This value is considerably lower than that of commonly used commercial hole transport materials, such as **Spiro-MeOTAD**. We believe these results suggest that polycyclic compounds based on the (hetero)fused furazano[3,4-*b*]pyrazine scaffold could serve as effective hole transport materials, as has been observed with previously described dibenzo[*f*,*h*]furazano[3,4-*b*]quinoxalines. Additionally, these compounds may provide a framework for designing new n-type semiconductors. However, this claim requires further research and experimental validation.

Supplementary Materials: The following supporting information can be downloaded at: https://www.mdpi.com/article/10.3390/electronicmat7030024/s1, Table S1: Optical micrographs of the surface of thin films of compounds **4a** and **4b** in different imaging modes, References relating to the Supplementary Materials file [37–39].

Author Contributions: Methodology, A.S.S., K.E.N. and A.V.I.; validation, A.S.S., E.M.K., Y.A.K. and P.A.S.; formal analysis, A.S.S., K.E.N. and A.V.I.; investigation, A.S.S., P.A.S., K.E.N. and A.V.I.; writing—original draft preparation, A.S.S., P.A.S. and E.V.V.; writing—review and editing, E.V.V. and V.N.C.; visualization, A.S.S.; supervision, I.A.W., E.V.V. and V.N.C.; project administration, E.V.V.; funding acquisition, V.N.C. All authors have read and agreed to the published version of the manuscript.

Funding: The research funding was received from the Ministry of Science and Higher Education of the Russian Federation within the framework of the state assignment (subject no. state. reg. 124020200024-9).

Data Availability Statement: The data presented in this study are available on request from the corresponding authors.

Acknowledgments: NMR and X-Ray experiments were carried out by using equipment of the Center for Joint Use "Spectroscopy and Analysis of Organic Compounds" at the Postovsky Institute of Organic Synthesis of the Ural Branch of the Russian Academy of Sciences.

Conflicts of Interest: The authors declare no conflicts of interest.

References

1. Bouachrine, M.; Ayachi, S. Organic electronics: Pioneering the future of sustainable and flexible technology. *RSC Adv.* **2025**, *15*, 45177–45195. [CrossRef] [PubMed]
2. Liu, C. Organic Electronics: Material Innovations, Synthesis Strategies, and Applications as Flexible Electronics. *Highlights Sci. Eng. Technol.* **2024**, *106*, 332–337. [CrossRef]
3. Jyoti Bala Kaushal, J.B.; Raut, P.; Kumar, S. Organic Electronics in Biosensing: A Promising Frontier for Medical and Environmental Applications. *Biosensors* **2023**, *13*, 976. [CrossRef] [PubMed]
4. Moiz, S.A.; Alshaikh, M.S.; Alahmadi, A.N.M. Organic Bioelectronics: Diversity of Electronics Along with Biosciences. *Biosensors* **2025**, *15*, 587. [CrossRef] [PubMed]
5. Gomez, R.; Souza, F.; Lima, R. Development of High-performance Organic Semiconductors for Flexible Electronics. *Res. Sci. Nat.* **2024**, *1*, 195–205. [CrossRef]
6. Zhao, Y.; Zhang, S.; Fan, Y.; Liu, Y.; Zhang, Y.; Jiang, L.; Wei, D. Multiscale Manufacturing of Organic Electronic Materials. *Adv. Mater.* **2026**, *38*, e09949. [CrossRef] [PubMed]
7. Liu, K.; Ouyang, B.; Guo, X. Advances in flexible organic field-effect transistors and their applications for flexible electronics. *npj Flex. Electron* **2022**, *6*, 1. [CrossRef]
8. Stępień, M.; Gońka, E.; Żyła, M.; Sprutta, N. Heterocyclic Nanographenes and Other Polycyclic Heteroaromatic Compounds: Synthetic Routes, Properties, and Applications. *Chem. Rev.* **2017**, *117*, 3479–3716. [CrossRef] [PubMed]
9. Borissov, A.; Maurya, Y.K.; Moshniaha, L.; Wong, W.-S.; Żyła-Karwowska, M.; Stępień, M. Recent Advances in Heterocyclic Nanographenes and Other Polycyclic Heteroaromatic Compounds. *Chem. Rev.* **2022**, *122*, 565–788. [CrossRef] [PubMed]
10. Pelliccioli, V.; Arnaboldi, S.; Cauteruccio, S. Phenanthrene-like Benzodichalcogenophenes: Synthesis, Electrochemical Behavior and Applications. *Molecules* **2026**, *31*, 425. [CrossRef] [PubMed]
11. Cheng, H.-C.; Ma, J.-L.; Guo, P.-H.; Shi, J.-C. Cyclization Synthetic Methodologies for Triphenylene Derivatives. *Chem. Asian J.* **2025**, *20*, e00809. [CrossRef] [PubMed]
12. Santra, S.; Khasanov, A.F.; Mukherjee, A.; Rahman, M.; Kovalev, I.S.; Kopchuk, D.S.; Zyryanov, G.V.; Majee, A.; Chupakhin, O.N.; Charushin, V.N. Mono- and Polyazatriphenylene-Based Ligands: An Updated Library of Synthetic Strategies (2001–2018). *New J. Chem.* **2021**, *45*, 20955–20971. [CrossRef]
13. Verbitskiy, E.V.; Rusinov, G.L.; Charushin, V.N. Diazatriphenylenes and their thiophene analogues: Synthesis and applications. *ARKIVOC* **2017**, *I*, 356–401. [CrossRef]
14. Verbitskiy, E.V.; Krynina, E.M.; Kvashnin, Y.A.; Charushin, V.N. 1,4-Diazatriphenylene and Its Hetero-Fused Analogs: Synthesis and Applications. *Molecules* **2026**, *31*, 2197. [CrossRef] [PubMed]
15. Kvashnin, Y.A.; Verbitskiy, E.V.; Rusinov, G.L.; Charushin, V.N. Modification and application of 1,2,5-oxadiazolo [3,4-*b*]pyrazine derivatives: Highlights and perspectives. *Russ. Chem. Bull.* **2022**, *71*, 1342–1362. [CrossRef]

16. Kvashnin, Y.A.; Slepukhin, P.A.; Gazizov, D.A.; Zhilina, E.F.; Rusinov, G.L.; Verbitskiy, E.V.; Charushin, V.N. (*E*)-2-(6-(4′-(Diphenylamino)-[1,1′-biphenyl]-2-yl)-[1,2,5]oxadiazolo [3,4-*b*]pyrazin-5(4*H*)-ylidene)-2-(6-(4′-(diphenylamino)-[1,1′-biphenyl]-2-yl)-[1,2,5]oxadiazolo [3,4-*b*]pyrazin-5-yl)acetonitrile. *Molbank* **2023**, *2023*, M1714. [CrossRef]
17. Verbitskiy, E.V.; Lipunova, G.N.; Nosova, E.V.; Charushin, V.N. Advances in the design of functionalized 1,4-diazines as components for photo- or/and electroactive materials. *Dye. Pigment.* **2023**, *220*, 111763. [CrossRef]
18. Verbitskiy, E.V.; Kvashnin, Y.A.; Medvedeva, M.V.; Svalova, T.S.; Kozitsina, A.N.; Eltsov, O.S.; Rusinov, G.L.; Charushin, V.N. First synthesis of new polycyclic systems from ortho-di(heteroaryl)-substituted furazanopyrazine derivatives by the Scholl reaction. *Mendeleev Commun.* **2022**, *32*, 722–725. [CrossRef]
19. Krynina, E.M.; Kvashnin, Y.A.; Gazizov, D.A.; Kodess, M.I.; Ezhikova, M.A.; Rusinov, G.L.; Verbitskiy, E.V.; Charushin, V.N. Two-step synthesis of new fused systems based on [1,2,5]oxadiazolo [3,4-*b*]quinoxaline by a combination of the Scholl reaction and nucleophilic aromatic substitution of hydrogen (S_N^H). *Russ. Chem. Bull.* **2024**, *73*, 1647–1658. [CrossRef]
20. Krynina, E.M.; Kvashnin, Y.A.; Zhilina, E.F.; Gazizov, D.A.; Slepukhin, P.A.; Rusinov, G.L.; Verbitskiy, E.V.; Charushin, V.N. [1,2,5]Oxadiazolo [3,4-*b*]dithieno [2,3-*f*:2′,3′-*h*]quinoxaline as a Versatile Scaffold for the Construction of Various Polycyclic Systems as Potential Organic Semiconductors. *Chemistry* **2025**, *7*, 158. [CrossRef]
21. Steparuk, A.S.; Kvashnin, Y.A.; Rusinov, G.L.; Verbitskiy, E.V.; Aleksandrov, A.E.; Lypenko, D.A.; Tameev, A.R.; Charushin, V.N. The first application of push-pull systems based on 1,2,5-oxadiazolo [3,4-*b*]pyrazine in organic light-emitting diodes and perovskite solar cells. *Russ. Chem. Bull.* **2023**, *72*, 527–533. [CrossRef]
22. Kvashnin, Y.A.; Krynina, E.M.; Medvedeva, M.V.; Svalova, T.S.; Kozitsina, A.N.; Eltsov, O.S.; Rusinov, G.L.; Verbitskiy, E.V.; Charushin, V.N. Synthesis of new polycyclic systems based on [1,2,5]chalcogenodiazolo [3,4-*b*]thieno [3,2-*h*]quinoxalines. *Russ. Chem. Bull.* **2023**, *72*, 939–947. [CrossRef]
23. Kvashnin, Y.A.; Verbitskiy, E.V.; Eltsov, O.S.; Slepukhin, P.A.; Tameev, A.R.; Nekrasova, N.V.; Rusinov, G.L.; Nunzi, J.-M.; Chupakhin, O.N.; Charushin, V.N. Dibenzo[*f*,*h*]furazano [3,4-*b*]quinoxalines: Synthesis by intramolecular cyclization through direct transition metal-free C–H functionalization and electrochemical, photophysical, and charge mobility characterization. *ACS Omega* **2020**, *5*, 8200–8210. [CrossRef] [PubMed]
24. Aukštuolis, A.; Girtan, M.; Mousdis, G.A.; Mallet, R.; Socol, M.; Rasheed, M.; Stanculescu, A. Measurement of charge carrier mobility in perovskite nanowire films by photo-CELIV method. *Proc. Rom. Acad. Ser. A Rom. Acad.* **2017**, *18*, 34−41.
25. Nakka, L.; Cheng, Y.; Aberle, A.G.; Lin, F. Analytical Review of Spiro-OMeTAD Hole Transport Materials: Paths Toward Stable and Efficient Perovskite Solar Cells. *Adv. Energy Sustain. Res.* **2022**, *3*, 2200045. [CrossRef]
26. Verbitskiy, E.V.; Charushin, V.N. The strategy of combined application of nucleophilic aromatic substitution of hydrogen (S_N^H) and transition metal-catalyzed cross-coupling reactions. *Mendeleev Commun.* **2025**, *35*, 493–502. [CrossRef]
27. Chung, D.D.L. Review graphite. *J. Mater. Sci.* **2002**, *37*, 1475−1489. [CrossRef]
28. Wu, J.; Pisula, W.; Müllen, K. Graphenes as potential material for electronics. *Chem. Rev.* **2007**, *107*, 718−747. [CrossRef] [PubMed]
29. Rudatia, P.S.; Mueller, D.C.; Meerholz, K. The *I-V* characteristics of organic hole-only devices based on crosslinked hole-transport layer. *J. Appl. Res. Technol.* **2015**, *13*, 253–260. [CrossRef]
30. Girotto, E.M.; Gazotti, W.A.; De Paoli, M.-A. Photoelectrochemical Properties of Poly(3,4-ethylenedioxythiophene). *J. Phys. Chem. B* **2000**, *104*, 6124–6127. [CrossRef]
31. Yook, K.S.; Lee, J.Y. Low driving voltage in organic light-emitting diodes using MoO_3 as an interlayer in hole transport layer. *Synth. Met.* **2009**, *159*, 69–71. [CrossRef]
32. Mott, N.F.; Gurney, R.W. *Electronic Processes in Ionic Crystals*; Oxford University Press: Oxford, UK, 1940. [CrossRef]
33. Anthony, J.E. The Larger Acenes: Versatile Organic Semiconductors. *Angew. Chem. Int. Ed.* **2008**, *47*, 452–483. [CrossRef] [PubMed]
34. Bunz, U.H.F.; Engelhart, J.U.; Lindner, B.D.; Schaffroth, M. Large *N*-Heteroacenes: New Tricks for Very Old Dogs? *Angew. Chem. Int. Ed.* **2013**, *52*, 2–14. [CrossRef] [PubMed]
35. Takimiya, K.; Shinamura, S.; Osaka, I.; Miyazaki, E. Thienoacene-Based Organic Semiconductors. *Adv. Mater.* **2011**, *23*, 4347–4370. [CrossRef] [PubMed]
36. Purushothama, U.; Narahari Sastry, G. Conjugate acene fused buckybowls: Evaluating their suitability for *p*-type, ambipolar and *n*-type air stable organic semiconductors. *Phys. Chem. Chem. Phys.* **2013**, *15*, 5039–5048. [CrossRef] [PubMed]
37. Dolomanov, O.V.; Bourhis, L.J.; Gildea, R.J.; Howard, J.A.K.; Puschmann, H. OLEX2: A Complete Structure Solution, Refinement and Analysis Program. *J. Appl. Cryst.* **2009**, *42*, 339–341. [CrossRef]
38. Sheldrick, G.M. SHELXT – Integrated space-group and crystal-structure determination. *Acta Cryst. A* **2015**, *71*, 3–8. [CrossRef] [PubMed]
39. Sheldrick, G.M. Crystal structure refinement with *SHELXL*. *Acta Cryst. C* **2015**, *71*, 3–8. [CrossRef] [PubMed]

Disclaimer/Publisher's Note: The statements, opinions and data contained in all publications are solely those of the individual author(s) and contributor(s) and not of MDPI and/or the editor(s). MDPI and/or the editor(s) disclaim responsibility for any injury to people or property resulting from any ideas, methods, instructions or products referred to in the content.